Tracing the Agulhas leakage with lead isotopes

Maxence Paul[1], Tina van de Flierdt[1], Mark Rehkämper[1], Roulin Khondoker[1], Dominik Weiss[1], Maeve C. Lohan[2], and William B. Homoky[3]

[1]Department of Earth Science and Engineering, Imperial College London, London, UK, [2]School of Geography, Earth, and Environmental Sciences, University of Plymouth, Plymouth, UK, [3]Department of Earth Sciences, University of Oxford, Oxford, UK

Abstract The transport of warm and salty waters from the Indian Ocean to the South Atlantic by the Agulhas Current constitutes a key return route of the meridional overturning circulation. Despite the importance of the Agulhas Leakage on interoceanic exchange, its role on biogeochemical cycles is poorly documented. Here we present the first lead (Pb) concentration and isotope data for surface seawater collected during the GEOTRACES cruise D357 in the Agulhas current system. Lead in surface waters of the Cape Basin is described by three distinct end-members: the South African coast, open South Atlantic seawater, and Indian Ocean seawater. The latter stands out in its Pb isotopic composition and can be tracked within two distinct Agulhas rings. High Pb concentrations in the Agulhas rings further corroborate an Indian Ocean provenance of waters and suggest that the Agulhas Leakage represents a major conduit not only for heat but also for trace metals.

1. Introduction

The Agulhas current is one of the largest currents of the Southern Hemisphere with a net transport of ~70 to 80 sverdrup (1 Sv = $10^6 m^3 s^{-1}$) [*Lutjeharms*, 2006]. It is the western boundary current of the Indian Ocean subtropical gyre and carries heat and salt from the Indian Ocean to the Atlantic Ocean (Figure 1), thereby making it a key player in compensating for the export of deep water from the North Atlantic in the global thermohaline circulation system [*Gordon et al.*, 1992; *Sloyan and Rintoul*, 2001]. Interoceanic exchange happens within the Agulhas Retroflection (Figure 1), an area where the Agulhas Current turns back toward the Indian Ocean, through detachment of eddies, rings, and filaments [*Lutjeharms*, 2006]. In this way, 5–8 Sv of warm and salty waters are leaked into the Atlantic Ocean [*de Ruijter et al.*, 1999].

The magnitude of this leakage is variable through time due to changes in the strength of the Agulhas Current and/or migration of the Subtropical Front. While several investigations have inferred increased leakage during warm (interglacial) periods and a reduced flux during cold (glacial) times [*Peeters et al.*, 2004; *Franzese et al.*, 2006; *Bard and Rickaby*, 2009], other studies indicate that reconstruction of salt leakage in this region on glacial-interglacial cycles is not straightforward [e.g., *Martínez-Méndez et al.*, 2010].

The Agulhas Leakage is an important pathway not only for salt and heat but also for biogeochemical cycles [e.g., *Villar et al.*, 2015]. In 2010, the first leg of the UK GEOTRACES transect GA10 occupied an area of the Cape Basin (Figure 1). A comprehensive sampling program was carried out, and here we present the first results on surface seawater lead (Pb) isotope compositions and concentrations from the southeastern Atlantic Ocean. The U-Th-Pb decay system is particularly suited for tracing the origin of trace metals in seawater, as Pb has three radiogenic (^{208}Pb, ^{207}Pb, and ^{206}Pb) isotopes and one primordial (^{204}Pb) nuclide, which allow effective tracing of natural and anthropogenic sources in the atmosphere-ocean-land system. Subnanomolar concentrations of Pb in seawater and the contamination-prone nature of this trace metal have, however, so far limited extensive use of the Pb isotope tracer in seawater [e.g., *Boyle et al.*, 2014].

2. Materials and Methods

Nineteen surface seawater samples were collected in the Cape Basin during the cruise D357, which sailed on the Royal Research Ship (RRS) Discovery from 18 October to 22 November 2010, representing the eastern part of the GEOTRACES GA10 transect along 40°S. Seawater samples were collected using a towed fish system (~3 m depth, portside) along two east-west transects from Cape Town out to 40°S and 5°W and back to Cape Town (Figure 1, Leg A: 18 October to 7 November 2010; samples 1A to 9A) and from Cape Town to
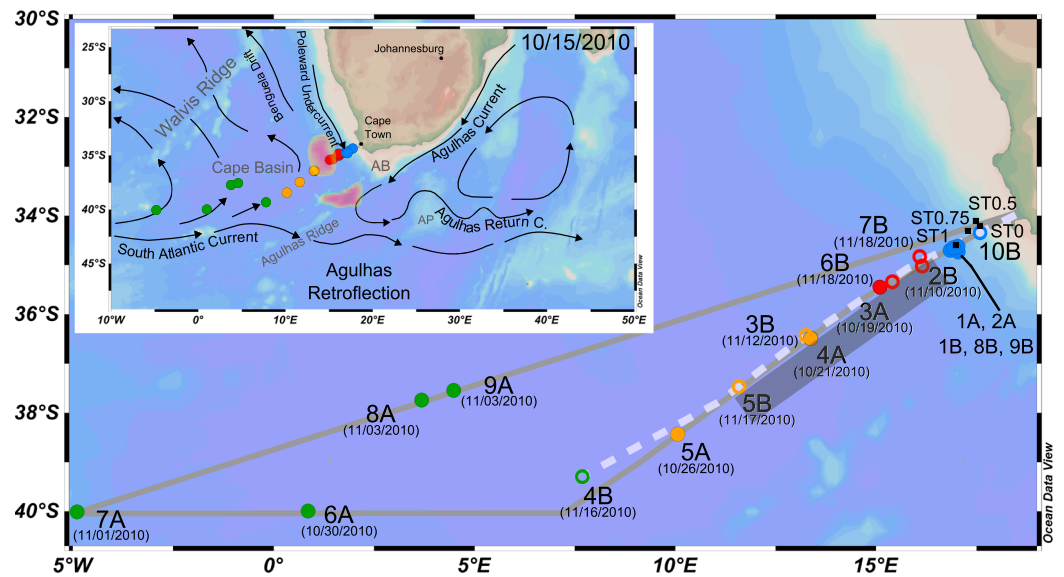
Figure 1. Inset: schematic circulation of surface and intermediate waters around South Africa (modified from *Richardson and Reverdin* [1987, and references therein]). Shaded areas highlight the core of two Agulhas rings on 15 October 2010 as suggested by sea surface height (SSH) anomalies obtained from satellite data (AVISO, http://www.aviso.oceanobs.com/ duacs/). An animation of the evolution of both rings is provided in the supporting information. AB refers to the Agulhas Bank; AP to the Agulhas Plateau. Large map: location of surface seawater samples collected during UK GEOTRACES GA10 cruise D357. Solid circles mark samples collected during Leg A (18 October to 7 November 2010); and open circles mark samples from Leg B (8 November to 22 November 2010). Cruise tracks are indicated by the grey solid (Leg A) and grey stippled line (Leg B) with sampling dates provided in brackets. Symbol colors (blue, red, yellow, and green) refer to the different groups of seawater Pb isotope compositions discussed in the text (coastal, Agulhas, transition, and open ocean; see also Figures 2 and 3). The grey solid rectangle represents the sample locations, which were directly influenced by the presence of the two distinct Agulhas rings. Small black squares off the South African coast mark the locations for collection of four seafloor sediment samples.

39°S and 7°W and back to Cape Town (Figure 1, Leg B: 8 November to 22 November 2010; samples 1B to 10B). Seawater was pumped directly into a trace metal clean laboratory van using a Teflon diaphragm pump connected to a clean, oil-free air compressor. Two 1 L samples were stored unfiltered in precleaned 1 L low-density polyethylene bottles and were acidified to pH 2 using distilled 6 *M* HCl between 2 and 12 weeks prior to analysis. Even though we did not carry out tests to determine the time needed for sample equilibration after acidification, we take the consistency of our results to indicate that the approach taken is valid (e.g., results presented here are part of a larger sample set).

The analyses were carried out following methods described in detail by *Paul et al.* [2015]. In brief, the Pb concentrations were determined by isotope dilution on 50 mL of seawater, while the Pb isotopic compositions were measured on 2 L seawater samples using a ^{207}Pb-^{204}Pb double spike. Following preconcentration and separation of Pb by Mg hydroxide coprecipitation and anion exchange chromatography, the purified Pb was loaded on single rhenium filaments with a silica gel activator and analyzed on a TRITON thermal ionization mass spectrometer in static mode using Faraday cups fitted with $10^{11} \, \Omega$ resistors. Two separate aliquots (i.e., unspiked and spiked) were analyzed for each sample, and the final data, corrected for instrumental mass fractionation, were obtained from these results using an iterative solver [*Rudge et al.*, 2009].

Total procedural blanks for concentration analyses were 12 ± 4 pg (1 standard deviation (SD)), representing between 4 and 9% of the natural sample Pb. Lead concentrations in all samples were corrected for this contribution. For the determination of Pb isotope compositions, the total procedural blank was 28 ± 21 pg (1 SD, *n* = 25). In all cases, this represents ≤1% of the indigenous Pb present in the sample, and no blank correction was performed for the isotope data.

Four seafloor sediment samples, collected across the South African shelf (Figure 1), were also analyzed for their bulk Pb isotope composition. Sampling and analysis protocols for these sediments are provided in the supporting information.
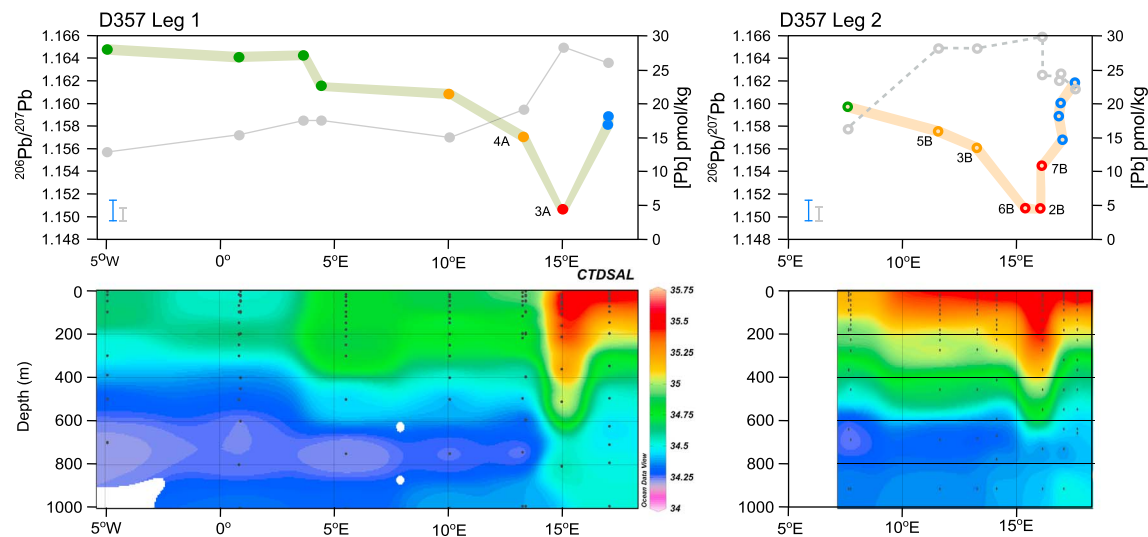
Figure 2. Zonal transects of Pb isotope composition (colored circles) and Pb concentration (grey circles) of surface seawater collected during Legs A (left) and Leg B (right) of cruise D357 along 40°S. Labels indicate sample names (see also Figure 1). Profiles are compared to salinity measurements from the same cruise for the uppermost 1000 m of the water column, visualized using Ocean Data View [Schlitzer, 2002].

3. Results

The Pb concentrations and isotopic compositions for surface seawater samples are illustrated in Figure 2 with their longitudinal coordinates to approximate distance from the South African coast. Lead contents range from 12 to 29 pmol/kg and reveal a trend of generally decreasing concentrations with increasing distance to the African continent (15 pmol/kg ± 2 pmol/kg, 1 SD, $n = 6$; between 5°W and 10°E = western part of the transect). Spatial evolution as well as absolute Pb concentrations described here are similar to results obtained in the area in the 1990s (28 pmol/kg ± 12, 1 SD) [Helmers and Rutgers van der Loeff, 1993]. A novel feature detected in our data set is that maximum Pb concentrations are confined in an offshore area between 11.5°E and 17.6°E (24 ± 3 pmol/kg, 1 SD, $n = 11$; Figure 2 and supporting information Table S1). These elevated Pb concentrations correspond to local maxima in salinity (Figure 2). Both the Pb concentrations and salinity levels indicate pronounced temporal variability in the shallow to intermediate water column, as samples from Legs A and B were collected less than 1 month apart, but display distinct features in hydrography and biogeochemistry (Figure 2).

The Pb isotope profiles for both cruise legs also display clear systematic variations, whereby the highest $^{206}Pb/^{207}Pb \approx 1.1647$ was observed in the sample collected most distal to the continent (Sample 7A, supporting information Table S1). In general, elevated ratios can be observed far offshore between 5°W and 5°E ($^{206}Pb/^{207}Pb = 1.1636 ± 14$ (1 SD), $^{208}Pb/^{207}Pb = 2.4357 ± 3$ (1 SD)), in good agreement with previously reported Pb isotope data for surface waters from the western part of the South Atlantic Subtropical Gyre ($^{206}Pb/^{207}Pb = 1.160 ± 9$, $^{208}Pb/^{207}Pb = 2.420 ± 65$) [Alleman et al., 2001a, 2001b]. Our coastal samples are characterized by moderately high $^{206}Pb/^{207}Pb$ values ($1.1591 ± 17$, 1 SD). A pronounced dip in the Pb isotope ratios of the surface waters is observed around 15°E with $^{206}Pb/^{207}Pb$ values as low as $1.1516 ± 19$ (1 SD) (Figure 2 and supporting information Table S1), coinciding with maxima in Pb concentrations and salinity.

4. Discussion

4.1. Deciphering the Pb Isotope Signal in the Southeastern Atlantic Ocean

In the three-isotope plot of Figure 3, our new surface seawater data show two clear trends, which are most likely generated by binary mixing involving three distinct end-members. This conclusion is supported by evaluating the results in diagrams of $^{208}Pb/^{204}Pb$ and $^{207}Pb/^{204}Pb$ versus $^{206}Pb/^{204}Pb$ (see supporting information). In general, the trace metal signature of surface waters in the Cape Basin can reflect either direct atmospheric or continental inputs (e.g., from proximal sources such as South Africa), or advection of water masses via ocean currents, which acquired their signature elsewhere. Satellite and salinity data (Figure 2 and supporting information Movie S1) reveal
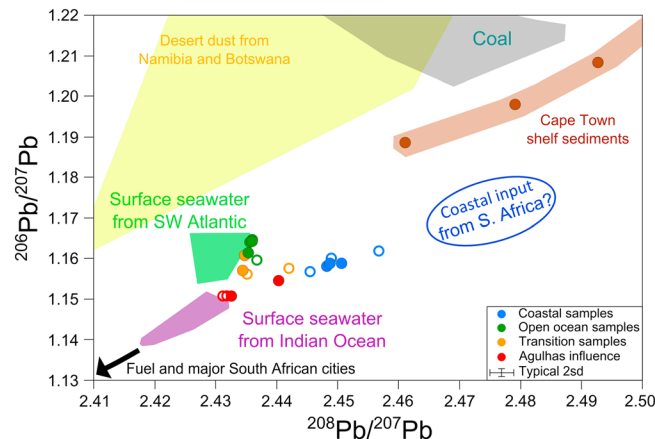
Figure 3. $^{206}Pb/^{207}Pb$ versus $^{208}Pb/^{207}Pb$ diagram showing the surface seawater samples analyzed for this study (solid and open circles for Legs A and B of cruise D357, respectively) and the three inferred end-members (open ocean South Atlantic seawater, Indian Ocean seawater, and coastal inputs from South Africa). Shelf sediments collected during cruise D357 are displayed with their Pb isotopic composition as brown circles. Additional colored fields illustrate literature data for potential sources of Pb to surface waters in the Southeastern Atlantic Ocean. The black arrow indicates that the Pb isotope composition for fuel and major South African cities extends beyond the lower left corner of the diagram (see text for further details). The 2 SD error bars are estimated from the long-term "external" reproducibility obtained in analyses of four in-house seawater reference samples [*Paul et al.*, 2015]. References for each field: surface seawater from Indian Ocean [*Lee et al.*, 2015], surface seawater from SW Atlantic [*Alleman et al.*, 2001b], fuel, and Johannesburg City [*Monna et al.*, 2006], Cape Town City [*Bollhöfer and Rosman*, 2000, 2002], coal [*Monna et al.*, 2006; *Díaz-Somoano et al.*, 2009], and desert dust [*Bollhöfer and Rosman*, 2000; *Kamber et al.*, 2010; *Vallelonga et al.*, 2010].

that during the sampling period two prominent Agulhas rings passed the area transporting warm and saline Indian Ocean waters into the Cape Basin. Here we suggest that Pb isotopes in the Cape Basin can be explained by the following three end-members: (i) a South African coastal signature, with high $^{206}Pb/^{207}Pb$ and $^{208}Pb/^{207}Pb$ ratios and relatively elevated Pb concentrations; (ii) open ocean South Atlantic seawater with high $^{206}Pb/^{207}Pb$, low $^{208}Pb/^{207}Pb$, and low Pb concentrations; and (iii) Indian Ocean seawater, with low $^{206}Pb/^{207}Pb$ and $^{208}Pb/^{207}Pb$ ratios, and the highest Pb concentrations.

Below we first briefly discuss the former two end-members to then focus on the significance of the latter in the context of the Agulhas Leakage.

4.2. Coastal Surface Seawater Off Southwestern Africa

Both Pb concentrations (21 to 25 pmol/kg) and isotopic signatures (e.g., $^{206}Pb/^{207}Pb \approx 1.1568$ to 1.1618) define a distinct group of coastal samples ($n = 6$) from east of 16.9°E (supporting information Table S1 and Figures 2 and 3). The proximity of this group to the coast suggests that South African sources are the major contributor of Pb to these samples, in agreement with previously published Pb studies [*Helmers and Rutgers van der Loeff*, 1993]. Dust propagation models [*Mahowald*, 2007] indicate that the South African coastal region is primarily influenced by dust from Africa rather than South America, with the latter being a major contributor of aerosols to the South Atlantic Ocean (see below).

The documented composition of anthropogenic emissions from major South African cities [*Bollhöfer and Rosman*, 2000; *Monna et al.*, 2006; *Witt et al.*, 2006], as measured before the phaseout of leaded gasoline in 2006 [*Monna et al.*, 2006], has much lower ratios of $^{206}Pb/^{207}Pb$ (≈ 1.08 to 1.19; Figure 3) and $^{208}Pb/^{207}Pb$ (≈ 2.34 to 2.37) than observed in the coastal seawater end-member. Hence, this seems unlikely as a major contributor to coastal seawater despite of the known importance of Pb remobilization from soil dust [*Díaz-Somoano et al.*, 2009]. Coal from South Africa should constitute an increasing share of anthropogenic Pb, since South African Pb emissions from coal have increased from ~300 t/yr in 1970 to ~1000 t/yr in 2010 [*Lee et al.*, 2014]. However, the $^{206}Pb/^{207}Pb$ ratio of coal is too high for a given $^{208}Pb/^{207}Pb$ to account for the Pb isotope signature observed in coastal seawater. In summary, strong contributions from industrial Pb sources to the coastal waters off South Africa seem unlikely. This conclusion is supported by the observation that Pb contents of surface seawater in the area have not changed significantly since the 1990s [*Helmers and Rutgers van der Loeff*, 1993], even though Pb emissions declined significantly between the 1990s and 2010 [*Lee et al.*, 2014].

Alternatively, deserts in Namibia and Botswana could represent a significant natural dust source for the South African coastal area [*Mahowald*, 2007]. Isotopic evaluation of this end-member, however, reveals a broad range of values (Figure 3). Such a broad range is unlikely to account for the well-defined linear trend described by the coastal seawater samples, in particular, because the effects of such dust contributions are mitigated by the low solubility of Pb from silicate phases in seawater [*Erel and Patterson*, 1994].

Sediments from the South African shelf, collected during the same cruise as the seawater samples (D357), display high $^{206}Pb/^{207}Pb$ and $^{208}Pb/^{207}Pb$ ratios (Figure 3, supporting information Table S2, and Text S1) that could, in principle, represent the coastal end-member. However, $^{206}Pb/^{207}Pb$ is too high and $^{208}Pb/^{206}Pb$ (not shown) too low to fit the well-defined trend of the seawater samples. It is conceivable that isotopic exchange between coastal seawater and shelf sediments may be responsible for this mismatch if such processes can produce an exchangeable Pb fraction that differs slightly in composition relative to the bulk sediment [e.g., *Lacan and Jeandel*, 2005; *Paul et al.*, 2011; *Lee et al.*, 2014]. However, in the absence of direct measurements to support such processes, contributions from other sources, such as uncharacterized local riverine inputs or submarine groundwater discharge, cannot be excluded.

4.3. Open Ocean Surface Seawater in the South Atlantic

The composition of open ocean surface seawater for the southeastern Atlantic Ocean (e.g., west off 7.6°E) determined here is very similar to historical data from the (south)western Atlantic Ocean [*Alleman et al.*, 2001a, 2001b]. Aerosols from major South American cities and natural dust sources [*Bollhöfer and Rosman*, 2000] overlap with the range of Pb isotope compositions defined by historical and our new seawater results. This suggests that Pb in the open South Atlantic is primarily dominated by aeolian inputs from South America. This conclusion is, furthermore, in agreement with dust propagation models [*Mahowald*, 2007], which indicate that dust transport via the westerlies from South America is the dominant source of dust to the South Atlantic. The similarity between the historical and our new seawater results (Figure 3) further implies that the Pb isotope composition of the South Atlantic Ocean has not changed significantly over the last 14 years, even though the Pb content and isotopic composition of the North Atlantic Ocean have evolved dramatically during this time, in response to the phaseout of leaded gasoline [*Boyle et al.*, 2014]. This contrast in temporal evolution is attributed to the limited exchange of aerosol-bound Pb between the Northern and Southern Hemispheres as a consequence of the Intertropical Convergence Zone and short residence time of Pb aerosols in the troposphere (<2 weeks) [*Alleman et al.*, 2001a].

4.4. Influence From the Indian Ocean-Agulhas Leakage

A key finding of our study is that the surface seawater samples display two distinct trends, which originate from the coastal and open Atlantic Ocean end-member, respectively, and converge in a well-defined offshore area (11.5°E to 17.6°E) at comparatively low $^{208}Pb/^{207}Pb$ and $^{206}Pb/^{207}Pb$ ratios (Figure 3). The Pb concentration and isotopic composition displayed by seawater in this geographical area implies an additional end-member beyond the South African and South American inputs discussed above. Elevated salinity data (Figure 2), as well as temperature and nutrient contents [*Wyatt et al.*, 2014] for the same seawater samples, mark the presence of Agulhas rings, which originate from the Agulhas Retroflection (Figure 1). The position of Agulhas rings during the time of the cruise can be reconstructed using sea surface height anomalies from satellite measurements [*van Ballegooyen et al.*, 1994] (Archiving, Validation, and Interpretation of Satellite (AVISO), http://www.aviso.oceanobs.com/duacs/). A movie is provided in the supporting information, which highlights that two prominent Agulhas rings influenced the region during the collection of our samples between mid-October and end of November 2010. The first Agulhas ring passed through the locations of samples 3A and 4A during Leg A and 2B, 6B, and 7B during Leg B. The second Agulhas ring moved northward in November 2010 and hence only affected the locations of samples 3B and 5B. In situ salinity measurements (Figure 2) show a large anomaly for samples 3A, 2B, 6B, and 7B, in agreement with the position of the first Agulhas ring. A comparison of the two salinity profiles (Figure 2) reveals a clear difference between the Legs A and B. The salinity anomaly of Leg B shows a larger spatial extent to the west of 14°E, which affects samples 3B, 5B, and corresponds to the satellite observation of the second Agulhas ring (supplementary Movie S1). Samples locations 3A, 4A, 2B, 3B, 5B, 6B, and 7B, which were affected by the presence of Agulhas rings, are marked by lower Pb isotope ratios and higher Pb concentrations, particularly locations 3A, 2B, and 6B (Figure 2). The latter characteristics can be matched to the Indian Ocean surface water signature recently reported by [*Lee et al.*, 2015], with [Pb] = 28 to 82 pmol/kg, $^{206}Pb/^{207}Pb$ = 1.1398 to 1.1502, and $^{208}Pb/^{207}Pb$ = 2.4188–2.4313. The high Pb content and distinct isotopic signature for some of our offshore samples is therefore entirely consistent with the presence of Agulhas rings in the Southeastern Atlantic Ocean, as revealed by both satellite observations and seawater salinity and temperature (Figures 2 and S1 in supporting information).

A detailed evaluation of the Pb isotope fingerprints for our seawater samples confirms that the lower ^{206}Pb/^{207}Pb and ^{208}Pb/^{207}Pb ratios of samples 3A, 2B, and 6B are consistent with advection of Indian Ocean waters in localized Agulhas rings. The Pb isotope data for samples 4A, 3B, 5B, and 7B point in the same direction but already show the effects of dilution with the prevailing ambient surface seawater (Figures 2 and 3). Hence, samples collected east of 16°E trend toward the South African coastal end-member, while seawater west of 7°E plots toward the open Atlantic Ocean signature. The observation that samples 2B and 7B, which were sampled at an almost identical location 8 days apart, have clearly distinct Pb isotope signatures and Pb contents (Figures 1 and 2) illustrates the highly transient nature of the short-lived Agulhas rings. Assuming a mean Pb concentration of 28 pmol/kg for the Agulhas rings and a water flux of 5 to 8 Sv for the Agulhas Leakage, this yields a Pb flux from the Indian to the South Atlantic of 0.9 to 1.5×10^9 g/yr. Notably, this Pb flux is equivalent to that provided by global atmospheric mineral dust deposition (1.6×10^9 g/yr, assuming 8% of Pb is released from dust to seawater) or major rivers such as the Ganges (1.8×10^9 g/yr) or the Mississippi (1.7×10^9 g/yr) [*Henderson and Maier-Reimer*, 2002]. It follows that the Agulhas system represents an important conveyor belt for the distribution of trace metals which will have an important impact on marine biogeochemical cycles.

5. Conclusion

The Pb isotope fingerprint of surface seawater from the Cape Basin describes two clear trends between three distinct end-members: (i) open ocean South Atlantic surface waters that carry an aerosol imprint from South American sources, (ii) coastal inputs from South Africa, and (iii) Indian Ocean water carried to the area within Agulhas rings. Lead isotopes and concentrations are excellent tracers of the transient occurrence of Agulhas rings, the exact path of which can be identified by satellite observations and confirmed by in situ hydrography measurements. Considering the significance of the Agulhas current on global heat transport, its Pb character-istics suggest it could also represent a significant conveyor for trace metals and their biogeochemical cycles.

References

Alleman, L. Y., T. M. Church, A. J. Véron, G. Kim, B. Hamelin, and A. R. Flegal (2001a), Isotopic evidence of contaminant lead in the South Atlantic troposphere and surface waters, *Deep Sea Res. Part II*, 48(13), 2811–2827.
Alleman, L. Y., T. M. Church, P. Ganguli, A. J. Véron, B. Hamelin, and A. R. Flegal (2001b), Role of oceanic circulation on contaminant lead distribution in the South Atlantic, *Deep Sea Res. Part II*, 48(13), 2855–2876, doi:10.1016/S0967-0645(01)00021-2.
Bard, E., and R. E. M. Rickaby (2009), Migration of the subtropical front as a modulator of glacial climate, *Nature*, 460(7253), 380–383, doi:10.1038/nature08189.
Bollhöfer, A., and K. J. R. Rosman (2000), Isotopic source signatures for atmospheric lead: The Southern Hemisphere, *Geochim. Cosmochim. Acta*, 64(19), 3251–3262, doi:10.1016/S0016-7037(00)00436-1.
Bollhöfer, A., and K. J. R. Rosman (2002), The temporal stability in lead isotopic signatures at selected sites in the Southern and Northern Hemispheres, *Geochim. Cosmochim. Acta*, 66(8), 1375–1386, doi:10.1016/S0016-7037(01)00862-6.
Boyle, E., et al. (2014), Anthropogenic lead emissions in the ocean: The evolving global experiment, *Oceanography*, 27(1), 69–75, doi:10.5670/oceanog.2014.10.
de Ruijter, W. P. M., A. Biastoch, S. S. Drijfhout, J. R. E. Lutjeharms, R. P. Matano, T. Pichevin, P. J. van Leeuwen, and W. Weijer (1999), Indian-Atlantic interocean exchange: Dynamics, estimation and impact, *J. Geophys. Res.*, 104(C9), 20,885–20,910, doi:10.1029/1998JC900099.
Díaz-Somoano, M., M. E. Kylander, M. A. López-Antón, I. Suárez-Ruiz, M. R. Martínez-Tarazona, M. Ferrat, B. Kober, and D. J. Weiss (2009), Stable lead isotope compositions in selected coals from around the world and implications for present day aerosol source tracing, *Environ. Sci. Technol.*, 43(4), 1078–1085, doi:10.1021/es801818r.
Erel, Y., and C. C. Patterson (1994), Leakage of industrial lead into the hydrocycle, *Geochim. Cosmochim. Acta*, 58(15), 3289–3296, doi:10.1016/0016-7037(94)90057-4.
Franzese, A. M., S. R. Hemming, S. L. Goldstein, and R. F. Anderson (2006), Reduced Agulhas Leakage during the Last Glacial Maximum inferred from an integrated provenance and flux study, *Earth Planet. Sci. Lett.*, 250(1–2), 72–88, doi:10.1016/j.epsl.2006.07.002.
Gordon, A. L., R. F. Weiss, W. M. Smethie, and M. J. Warner (1992), Thermocline and intermediate water communication between the south Atlantic and Indian oceans, *J. Geophys. Res.*, 97(C5), 7223–7240, doi:10.1029/92JC00485.
Helmers, E., and M. M. Rutgers van der Loeff (1993), Lead and aluminum in Atlantic surface waters (50°N to 50°S) reflecting anthropogenic and natural sources in the eolian transport, *J. Geophys. Res.*, 98, 20,261–20,732, doi:10.1029/93JC01623.
Henderson, G. M., and E. Maier-Reimer (2002), Advection and removal of 210Pb and stable Pb isotopes in the oceans: A general circulation model study, *Geochim. Cosmochim. Acta*, 66(2), 257–272, doi:10.1016/S0016-7037(01)00779-7.
Kamber, B. S., S. K. Marx, and H. A. McGowan (2010), Comment on "Lead isotopic evidence for an Australian source of Aeolian dust to Antarctica at times over the last 170,000 years" by P. De Deckker, M. Norman, I.D. Goodwin, A. Wain and F.X. Gingele [Palaeogeography, Palaeoclimatology, Palaeoecology 285 (2010)205–223], *Palaeogeogr. Palaeoclimatol. Palaeoecol.*, 298(3–4), 432–436, doi:10.1016/j.palaeo.2010.06.024.
Lacan, F., and C. Jeandel (2005), Neodymium isotopes as a new tool for quantifying exchange fluxes at the continent–ocean interface, *Earth Planet. Sci. Lett.*, 232(3–4), 245–257, doi:10.1016/j.epsl.2005.01.004.
Lee, J.-M., E. A. Boyle, I. Suci Nurhati, M. Pfeiffer, A. J. Meltzner, and B. Suwargadi (2014), Coral-based history of lead and lead isotopes of the surface Indian Ocean since the mid-20th century, *Earth Planet. Sci. Lett.*, 398, 37–47, doi:10.1016/j.epsl.2014.04.030.
Lee, J.-M., E. A. Boyle, T. Gamo, H. Obata, K. Norisuye, and Y. Echegoyen (2015), Impact of anthropogenic Pb and ocean circulation on the recent distribution of Pb isotopes in the Indian Ocean, *Geochim. Cosmochim. Acta*, doi:10.1016/j.gca.2015.08.013.

Lutjeharms, J. R. E. (2006), *The Agulhas Current*, Springer, Berlin.

Mahowald, N. M. (2007), Anthropocene changes in desert area: Sensitivity to climate model predictions, *Geophys. Res. Lett.*, *34*, L18817, doi:10.1029/2007GL030472.

Martínez-Méndez, G., R. Zahn, I. R. Hall, F. J. C. Peeters, L. D. Pena, I. Cacho, and C. Negre (2010), Contrasting multiproxy reconstructions of surface ocean hydrography in the Agulhas Corridor and implications for the Agulhas Leakage during the last 345,000 years, *Paleoceanography*, *25*, PA4227, doi:10.1029/2009PA001879.

Monna, F., M. Poujol, R. Losno, J. Dominik, H. Annegarn, and H. Coetzee (2006), Origin of atmospheric lead in Johannesburg, South Africa, *Atmos. Environ.*, *40*(34), 6554–6566, doi:10.1016/j.atmosenv.2006.05.064.

Paul, M., L. Reisberg, N. Vigier, and C. France-Lanord (2011), Behavior of osmium at the freshwater/saltwater interface based on Ganga derived sediments from the estuarine zone, *Geochem. Geophys. Geosyst.*, *12*, Q12023, doi:10.1029/2011GC003831.

Paul, M., L. Bridgestock, M. Rehkämper, T. van DeFlierdt, and D. Weiss (2015), High-precision measurements of seawater Pb isotope compositions by double spike thermal ionization mass spectrometry, *Anal. Chim. Acta*, *863*, 59–69, doi:10.1016/j.aca.2014.12.012.

Peeters, F. J. C., R. Acheson, G.-J. A. Brummer, W. P. M. de Ruijter, R. R. Schneider, G. M. Ganssen, E. Ufkes, and D. Kroon (2004), Vigorous exchange between the Indian and Atlantic Oceans at the end of the past five glacial periods, *Nature*, *430*(7000), 661–665, doi:10.1038/nature02785.

Richardson, P. L., and G. Reverdin (1987), Seasonal cycle of velocity in the Atlantic North Equatorial Countercurrent as measured by surface drifters, current meters, and ship drifts, *J. Geophys. Res.*, *92*(C4), 3691–3708, doi:10.1029/JC092iC04p03691.

Rudge, J. F., B. C. Reynolds, and B. Bourdon (2009), The double spike toolbox, *Chem. Geol.*, *265*(3–4), 420–431.

Schlitzer, R. (2002), Ocean data view. [Available at http://www.awi-bremerhaven.de/GEO/ODV(2002).]

Sloyan, B. M., and S. R. Rintoul (2001), Circulation, renewal, and modification of Antarctic mode and intermediate water*, *J. Phys. Oceanogr.*, *31*(4), 1005–1030, doi:10.1175/1520-0485(2001)031<1005:CRAMOA>2.0.CO;2.

The GEOTRACES Group (2015), The GEOTRACES intermediate data product 2014, *Mar. Chem.*, doi:10.1016/j.marchem.2015.04.005.

Vallelonga, P., et al. (2010), Lead isotopic compositions in the EPICA Dome C ice core and Southern Hemisphere potential source areas, *Quat. Sci. Rev.*, *29*(1–2), 247–255, doi:10.1016/j.quascirev.2009.06.019.

van Ballegooyen, R. C., M. L. Gründlingh, and J. R. E. Lutjeharms (1994), Eddy fluxes of heat and salt from the southwest Indian Ocean into the southeast Atlantic Ocean: A case study, *J. Geophys. Res.*, *99*(C7), 14,053–14,070, doi:10.1029/94JC00383.

Villar, E., et al. (2015), Environmental characteristics of Agulhas rings affect interocean plankton transport, *Science*, *348*(6237), 1261447, doi:10.1126/science.1261447.

Witt, M., A. R. Baker, and T. D. Jickells (2006), Atmospheric trace metals over the Atlantic and South Indian Oceans: Investigation of metal concentrations and lead isotope ratios in coastal and remote marine aerosols, *Atmos. Environ.*, *40*(28), 5435–5451, doi:10.1016/j.atmosenv.2006.04.041.

Wyatt, N. J., A. Milne, E. M. S. Woodward, A. P. Rees, T. J. Browning, H. A. Bouman, P. J. Worsfold, and M. C. Lohan (2014), Biogeochemical cycling of dissolved zinc along the GEOTRACES South Atlantic transect GA10 at 40°S, *Global Biogeochem. Cycles*, *28*, 44–56, doi:10.1002/2013GB004637.